Arch. Rational Mech. Anal. 212 (2014) 683–706
Digital Object Identifier (DOI) 10.1007/s00205-013-0717-6

On Finite Time Singularity and Global Regularity of an Axisymmetric Model for the 3D Euler Equations

Thomas Y. Hou, Zhen Lei, Guo Luo, Shu Wang & Chen Zou

Communicated by V. Šverák

Abstract

In (Comm Pure Appl Math 62(4):502–564, 2009), Hou and Lei proposed a 3D model for the axisymmetric incompressible Euler and Navier–Stokes equations with swirl. This model shares a number of properties of the 3D incompressible Euler and Navier–Stokes equations. In this paper, we prove that the 3D inviscid model with an appropriate Neumann-Robin or Dirichlet-Robin boundary condition will develop a finite time singularity in an axisymmetric domain. We also provide numerical confirmation for our finite time blowup results. We further demonstrate that the energy of the blowup solution is bounded up to the singularity time, and the blowup mechanism for the mixed Dirichlet-Robin boundary condition is essentially the same as that for the energy conserving homogeneous Dirichlet boundary condition. Finally, we prove that the 3D inviscid model has globally smooth solutions for a class of large smooth initial data with some appropriate boundary condition. Both the analysis and the results we obtain here improve the previous work in a rectangular domain by Hou et al. (Adv Math 230:607–641, 2012) in several respects.

1. Introduction

Whether the 3D incompressible Euler or Navier–Stokes equations can develop a finite time singularity from smooth initial data with finite energy is one of the most challenging questions in nonlinear partial differential equations [13]. There have been many previous studies devoted to this challenging question, see e.g. [5–7,9–11,28] and three recent review articles [1,8,18]. There have been a number of attempts to investigate the possible finite time singularity formation of the 3D Euler equations through numerical computations, see e.g. [3,15–17,25,29,31]. Most of the previous studies on finite time singularity have been inconclusive [18–20]. However, the recent work of Luo and Hou in [27] presents convincing numerical evidence that the 3D axisymmetric Euler equations can indeed develop a finite time

singularity. The presence of the boundary and the specially designed symmetry of the initial condition seem to play a crucial role in generating this highly anisotropic singularity that is not of Leray type.

In [21], Hou and Li investigated the stabilizing effect of convection via an exact 1D model. They found that the convection term plays an essential role in canceling the destabilizing vortex stretching terms in this 1D model. This observation enabled them to obtain a pointwise estimate via a Lyapunov function which controls the dynamic growth of the derivative of vorticity. Motivated by the work of [21], Hou and Lei further investigated the role of convection by constructing the following 3D model of the axisymmetric Navier–Stokes equations with swirl [22]:

$$\begin{cases} \partial_t u = \nu \left(\partial_r^2 + \frac{3}{r}\partial_r + \partial_z^2\right) u + 2u\partial_z \psi, \\ \partial_t \omega = \nu \left(\partial_r^2 + \frac{3}{r}\partial_r + \partial_z^2\right) \omega + \partial_z (u^2), \\ -\left(\partial_r^2 + \frac{3}{r}\partial_r + \partial_z^2\right) \psi = \omega. \end{cases} \tag{1.1}$$

When $\nu = 0$, we refer to the above model as the 3D inviscid model. This model is derived by using a reformulated Navier–Stokes equations in terms of a set of new variables $(u, \omega, \psi) = (u^\theta, \omega^\theta, \psi^\theta)/r$, where $r = \sqrt{x_1^2 + x_2^2}$, u^θ is the angular velocity, ω^θ the angular vorticity, and ψ^θ the angular stream function, see [21, 22]. The only difference between this 3D model and the reformulated Navier–Stokes equations is that we neglect the convection term in the model. This new 3D model shares several well known properties of the full 3D Euler or Navier–Stokes equations [22]. These include an energy identity for smooth solutions, a non-blowup criterion of Beale–Kato–Majda type [2], a non-blowup criterion of Prodi–Serrin type [30,32], and a partial regularity result for the model [23], which is an analogue of the Caffarelli–Kohn–Nirenberg theory [4,26] for the full Navier–Stokes equations.

Despite the striking similarity at the theoretical level, this 3D model seems to have a very different behavior from that of the Euler or Navier–Stokes equations. Numerical study in [22] seems to indicate that the model develops a potential finite time singularity from smooth initial data with finite energy. In a recent paper [24], Hou, Shi, and Wang proved that the inviscid model can develop a finite time singularity for a class of smooth initial data with a Neumann-Robin boundary condition. The analysis in [24] was carried out for a rectangular domain and does not apply to the axisymmetric domain considered in this paper.

In this paper, we prove that the 3D inviscid model with an appropriate boundary condition of Neumann-Robin type can develop a finite time singularity starting from smooth initial data on a bounded or an unbounded exterior axisymmetric domain. The analysis in the axisymmetric unbounded domain presents several new difficulties. First of all, the local well-posedness of the initial boundary value problem requires an elliptic regularity estimate on a domain with corner. By assuming that the initial value of u satisfies an appropriate condition at the corner, we can show that ω satisfies certain compatibility condition at the corner as long as the solution remains smooth. Using this compatibility condition on ω, we can recover the classical elliptic estimate for ψ in terms of ω in the special domain with corner that we consider here.

The analysis of proving finite time singularity is more complicated in the case of an axisymmetric unbounded exterior domain. In the previous work in [24], the first eigenfunction of the Laplacian operator in a rectangular domain is positive and can be written explicitly as a tensor product of one-dimensional sine functions. In the case of an unbounded exterior domain, a positive decaying eigenfunction of the Laplacian operator does not seem to exist. This requires us to come up with a new method of analysis. The new method of analysis is based on a delicate balance of different integral quantities that we try to control. Using this analysis, we can find a relatively large class of positive decaying test functions that we can use to obtain a desired nonlinear differential inequality, leading to finite time blowup. Such method of analysis is more general than the one presented in [24]. It may find applications in analyzing finite time blowup of other nonlinear PDEs.

The results we obtain in this paper improve those in [24] in several respects. First of all, we remove the positivity condition of an integral quantity involving the logarithm of the initial condition, i.e. $\log(u_0^2)$. This positivity condition poses a severe constraint on the kind of initial data that could develop a finite time singularity. By removing this condition on u_0, our blowup results apply to a much larger class of initial data than those considered in [24]. Our numerical experiments suggest that if one imposes the positivity condition on this integral quantity at $t = 0$, the energy tends to increase rapidly in time and may become unbounded at the singularity time. However, if we choose an initial condition u_0 such that this integral quantity is negative and large in amplitude, then the energy grows very slowly in time and remains bounded at the singularity time. The second improvement is that we establish the global regularity of the 3D model for a class of initial boundary value problem with large initial data, while the previous result in [24] requires some smallness condition on the initial data.

To confirm the analytical results on the finite time blowup of the 3D model, we have performed well-resolved adaptive computations of the 3D model with axisymmetric initial and boundary data that satisfy the conditions of our theorems. For the initial condition we consider here, we demonstrate that the energy remains bounded up to the singularity time. Thus, the finite time blowup of the 3D model is not driven by infinite energy. Moreover, we repeat the computation using the same initial condition, but changing the boundary condition from the mixed Dirichlet-Robin boundary condition to the energy conserving homogeneous Dirichlet boundary condition for ψ. We find that the mechanism for finite time blowup of the mixed Dirichlet-Robin boundary condition is essentially the same as that of the energy conserving homogeneous boundary condition.

It is worth pointing out that the point of singularity for the 3D axisymmetric Euler equations reported in [27] coincides with a stagnation point of the flow at the boundary $r = 1$ where the effect of convection is minimized. This is consistent with the main message conveyed in [21,22,24] and the current paper. If one can treat the convection term as a small perturbation to the 3D Euler equation, the analysis presented in this paper may shed some light to the understanding of the mechanism of singularity formation of the 3D Euler equation.

The paper is organized as follows. In Section 2 we will state our main results and present our main ideas of their proofs. Section 3 is devoted to proving the finite

time singularity of the 3D inviscid model. In Section 4, we present some numerical evidence for finite time blowup of the 3D model, confirming our theoretical results. We present our global well-posedness result in Section 5. The local well-posedness of the initial boundary value problem is discussed in Appendix A.

2. Main Results

In this section we set up our problem and state our main results. First of all, let us recall that the 3D model (1.1) is formulated in terms of a set of new variables $u = u^\theta/r, \omega = \omega^\theta/r, \psi = \psi^\theta/r$. Due to this change of variables, the original three-dimensional Laplacian operator for ψ^θ is changed to a five-dimensional Laplacian operator for ψ in the axisymmetric cylindrical coordinate in (1.1). Thus we can reformulate our 3D inviscid model in the three-dimensional axisymmetric cylindrical domain

$$D(\gamma_1, \gamma_2) = \left\{(x_1, x_2, z) \in \mathbb{R}^3 : \gamma_1 \leqq r = \sqrt{x_1^2 + x_2^2} < \gamma_2; 0 \leqq z \leqq 1\right\}$$

as a five-dimensional problem in the axisymmetric cylindrical domain

$$\Omega(\gamma_1, \gamma_2) = \left\{ (x_1, \ldots, x_4, z) \in \mathbb{R}^5 : \gamma_1 \leqq r = \left(\sum_{j=1}^{4} x_j^2\right)^{\frac{1}{2}} < \gamma_2; 0 \leqq z \leqq 1 \right\}.$$

It is much more convenient to perform the well-posedness and the finite time blowup analysis for our 3D model in the five-dimensional setting. In the remaining part of the paper, we will carry out our analysis in this axisymmetric five-dimensional domain.

Denote

$$S_{\text{exterior}} \equiv \left\{ \beta > 0 \quad | \quad \beta \neq \frac{k \int_0^\infty \mathrm{e}^{-k\cosh(\theta)} \cosh^2(\theta)\, \mathrm{d}\theta}{\int_0^\infty \mathrm{e}^{-k\cosh(\theta)} \cosh(\theta)\, \mathrm{d}\theta}, \ \forall k \in \mathbb{Z}^+ \right\}. \tag{2.1}$$

Now we are ready to state the first result of this paper which is concerned with the local well-posedness of classical solutions to the 3D inviscid model with a Neumann-Robin type boundary condition on the exterior domain $\Omega(1, \infty)$.

Theorem 2.1. *Let S_{exterior} be defined in (2.1) and $\beta \in S_{\text{exterior}}$. Consider the initial-boundary value problem of the 3D model (1.1) with the initial data*

$$u_0 \in H^3(\Omega(1, \infty)), \quad \psi_0 \in H^4(\Omega(1, \infty)), \tag{2.2}$$

and the Neumann-Robin type boundary condition

$$(\psi_r + \beta\psi)|_{r=1} = 0, \quad \psi_z|_{z=0} = 0, \quad \psi_z|_{z=1} = 0. \tag{2.3}$$

Further, we assume that $u_0^2 > 0$ for $0 < z < 1$, $u_0|_{z=0,1} = u_{0z}|_{z=0,1} = \psi_{0z}|_{z=0,1} = 0$, and $(\psi_{0r} + \beta\psi_0)|_{r=1} = 0$. Then there exists a unique smooth solution (u, ψ) to the 3D inviscid model with the initial data (2.2) and the boundary condition (2.3) on $[0, T)$ for some $T > 0$. Moreover, we have

$$u \in C([0, T), H^3(\Omega(1, \infty))), \quad \psi \in C([0, T), H^4(\Omega(1, \infty))). \tag{2.4}$$

The proof of Theorem 2.1 relies on an important property of the elliptic operator with the mixed Neumann-Robin type boundary condition. Note that the boundary condition in (2.3) is not the third type. To recover the standard elliptic regularity estimate, we need to study the spectral property of the differential operator which requires that $\beta \in S_{\text{exterior}}$. The condition $\beta \in S_{\text{exterior}}$ can be also understood as a special case of the classical necessary and sufficient condition for solvability of an elliptic equation in terms of the kernel of the adjoint operator.

Next, we state the finite time blowup result of the exterior problem (1.1), (2.2) and (2.3).

Theorem 2.2. *Suppose that all the assumptions in Theorem 2.1 are satisfied. Let* $\beta \geqq 2 + 2\sqrt{1 + \frac{\pi^2}{4}}, \alpha = \frac{\beta}{2}$ *and*

$$\phi(r, z) = \theta(r)\sin(\pi z),\ \theta(r) = \mathrm{e}^{-\alpha r^2}, \quad \Phi(r, z) = \phi_{rr} + \frac{3}{r}\phi_r + \phi_{zz}. \tag{2.5}$$

Then the solution of the 3D inviscid model will develop a finite time singularity in the H^3 *norm provided that* $\int_0^1 \int_1^\infty \Phi \log(u_0^2) r^3 \,\mathrm{d}r\,\mathrm{d}z$ *is finite and* $\int_0^1 \int_1^\infty \Phi \psi_{0z} r^3 \,\mathrm{d}r\,\mathrm{d}z$ *is positive.*

To prove Theorem 2.2, we need to construct a special positive test function that satisfies certain properties. In the case of a rectangular domain, one can simply take the product of sine functions in the xy-domain as a testing function. In the case of an unbounded exterior domain in the axisymmetric geometry, a positive and decaying eigenfunction of the Laplacian operator does not seem to exist. This requires us to develop a new method of analysis. We will present the details of the proof of Theorem 2.2 in Section 3.

Remark 2.1. We remark that Theorems 2.1 and 2.2 can be also generalized to the bounded domain case $\Omega(0, 1)$. We will not present this result here.

Remark 2.2. When β is small, we can prove that the energy of the initial boundary value problem that we consider here will be bounded as long as the solution remains smooth (see Proposition 2.1 in [24]).

Our next theorem concerns the local well-posedness and finite time blowup of the 3D inviscid model in a bounded axisymmetric domain $\Omega(0, 1)$.

Let $(\lambda_k, \theta_k(r))$ $(k = 1, 2, \ldots)$ be the eigenvalue–eigenfunction pair of the following Dirichlet eigenvalue problem:

$$\begin{cases} -\left(\partial_r^2 + \frac{3}{r}\partial_r\right)\theta_k = \lambda_k \theta_k, \quad r \in [0, 1), \\ \theta_k|_{r=1} = 0. \end{cases} \tag{2.6}$$

Define

$$S_{\text{interior}} \equiv \left\{ \beta > 0 \mid \beta \neq \lambda_k, \beta \neq \frac{\sqrt{\lambda_k}(\mathrm{e}^{\sqrt{\lambda_k}} + \mathrm{e}^{-\sqrt{\lambda_k}})}{\mathrm{e}^{\sqrt{\lambda_k}} - \mathrm{e}^{-\sqrt{\lambda_k}}} \text{ for all } k = 1, 2, \ldots \right\}, \tag{2.7}$$

and

$$\phi(r,z) = \frac{\mathrm{e}^{-\alpha(z-1)} + \mathrm{e}^{\alpha(z-1)}}{2}\theta_1(r). \tag{2.8}$$

Moreover, we assume that α, β satisfy

$$0 < \alpha < \sqrt{\lambda_1}, \quad \beta = \frac{\lambda_1}{\alpha}\frac{\mathrm{e}^{\alpha} - \mathrm{e}^{-\alpha}}{\mathrm{e}^{\alpha} + \mathrm{e}^{-\alpha}} > \sqrt{\lambda_1}\left(\frac{\mathrm{e}^{\sqrt{\lambda_1}} + \mathrm{e}^{-\sqrt{\lambda_1}}}{\mathrm{e}^{\sqrt{\lambda_1}} - \mathrm{e}^{-\sqrt{\lambda_1}}}\right). \tag{2.9}$$

We can prove the following local-well-posedness and finite time blowup results.

Theorem 2.3. *(A) Local well-posedness. Let* S_{interior} *be defined in* (2.7) *and* $\beta \in S_{\text{interior}}$. *Consider the initial-boundary value problem of the 3D model* (1.1) *with the initial data* $u_0 \in H^3(\Omega(0,1))$, $\psi_0 \in H^4(\Omega(0,1))$ *and the Dirichlet-Robin type boundary condition*

$$\psi|_{r=1} = 0, \quad \psi|_{z=1} = 0, \quad (\psi_z + \beta\psi)|_{z=0} = 0. \tag{2.10}$$

Furthermore, we assume that

$$u_0|_{z=0,1} = 0,\ u_0|_{r=1} = 0,\ \psi_0|_{z=1} = 0,\ (\psi_{0z} + \beta\psi_0)|_{z=0} = 0,\ \psi_0|_{r=1} = 0. \tag{2.11}$$

Then there exists a unique smooth solution (u, ψ) *to the 3D inviscid model with the initial data* (2.11) *and the boundary condition* (2.10) *on* $[0, T)$ *for some* $T > 0$. *Moreover, we have*

$$u \in C([0,T), H^3(\Omega(0,1))), \quad \psi \in C([0,T), H^4(\Omega(0,1))). \tag{2.12}$$

(B) Finite time blowup. Suppose (2.9) *is satisfied and* $u_0^2 > 0$ *for* $0 < z < 1$. *Let* Φ *be defined as in* (2.5). *If* $\int_0^1\int_0^1 (\log u_0^2)\Phi r^3 \mathrm{d}r\mathrm{d}z$ *is finite and* $\int_0^1\int_0^1 \psi_{0z}\Phi r^3\mathrm{d}r\mathrm{d}z$ *is positive, then the solution of the 3D inviscid model will develop a finite time singularity in the* H^3 *norm.*

Theorem 2.3 can be proved by following an argument similar to that in [24]. We just need to replace the first eigenfunction $\sin\pi x_1 \sin\pi x_2 \sin\pi x_3 \sin\pi x_4$ of the rectangular domain by the first eigenfunction $\phi_1(x)$ of the unit ball in $\mathbb{R}^4$. We will omit the proof of Theorem 2.3 in this paper.

The last theorem concerns the global well-posedness of a class of initial boundary value problems in the axisymmetric domain $\Omega(0,1)$. The most interesting aspect of this result is that the initial condition can be made as large as we wish in the Sobolev space. This is achieved by effectively imposing the boundary condition for $\partial_z\psi|_{\partial\Omega(0,1)} = -M$ with M being a large positive constant.

Theorem 2.4. *Let* $M > 0$ *and* $s \geqq 3$. *Assume that* $u_0 \in H^s(\Omega(0,1))$, $\psi_0 \in H^{s+1}(\Omega(0,1))$ *with* $\partial_z^k u_0|_{z=0} = \partial_z^k u_0|_{z=1} = 0$ *for all integers* $k = 0, \ldots, [\frac{s-3}{2}]+1$ *and* $\psi_0|_{r=1} = -Mz$, $\partial_z\psi_0|_{z=0} = \partial_z\psi_0|_{z=1} = -M$. *Then the 3D inviscid model with the initial and boundary data*

$$u(0,\cdot) = u_0(\cdot), \quad \psi(0,\cdot) = \psi_0(\cdot), \tag{2.13}$$

and

$$\psi(t,1,z) = -Mz,\ \partial_z\psi(t,r,0) = \partial_z\psi(t,r,1) = -M \tag{2.14}$$

admits a unique global smooth solution (u,ψ) *with* $u \in C([0,\infty); H^s(\Omega(0,1)))$, $\psi \in C([0,\infty); H^{s+1}(\Omega(0,1)))$ *provided that*

$$\|\nabla\partial_z\psi_0\|_{H^{s-1}} \leqq \frac{M}{8C_s^2},\quad \|u_0^2\|_{H^s} \leqq \frac{M^2}{4C_s^3}, \tag{2.15}$$

where C_s *is an absolute positive constant depending on* s *and* Ω *only. Moreover, we have*

$$\|u(t)^2\|_{H^s(\Omega(0,1))} \leq C_s\|u_0^2\|_{H^s(\Omega(0,1))}\mathrm{e}^{-2Mt}, \tag{2.16}$$

and

$$\|\nabla\partial_z\psi\|_{H^{s-1}(\Omega(0,1))} \leq \|\nabla\partial_z\psi_0\|_{H^{s-1}(\Omega(0,1))} + \frac{C_s}{2M}\|u_0^2\|_{H^s(\Omega(0,1))}. \tag{2.17}$$

We will present the proof of Theorem 2.4 in Section 5.

3. Finite Time Singularity in the Exterior Domain

In this section, we present the proof of Theorem 2.2, which shows that the 3D inviscid model develops a finite time singularity in the exterior domain.

Proof of Theorem 2.2. We will prove Theorem 2.2 by contradiction, as in [24]. By the local well-posedness result, we know that the initial boundary value problem of the 3D inviscid model has a unique solution $u \in H^3(\Omega(1,\infty))$ and $\psi \in H^4(\Omega(1,\infty))$ for $0 \leqq t \leqq T$ for some $T > 0$. Let T_b be the largest time for which our 3D inviscid model has a unique smooth solution $u \in H^3(\Omega)$ and $\psi \in H^4(\Omega)$ for $0 \leqq t < T_b$. We will prove that $T_b < \infty$. Suppose that $T_b = \infty$. Then we have

$$u \in C([0,\infty), H^3(\Omega(1,\infty))),\quad \psi \in C([0,\infty), H^4(\Omega(1,\infty))). \tag{3.1}$$

We will prove that (3.1) would lead to a contradiction.

Define ϕ and Φ as in Theorem 2.2. By a straightforward calculation, we have

$$\Phi(r,z) = [4\alpha^2r^2 - (8\alpha+\pi^2)]\phi(r,z). \tag{3.2}$$

For $\alpha \geqq 1 + \sqrt{1+\frac{\pi^2}{4}}$, it is easy to get that

$$4\alpha^2r^2 - (8\alpha+\pi^2) \geqq 4\alpha^2 - (8\alpha+\pi^2) \geqq 0 \quad \text{for } r \geqq 1.$$

Consequently, we have

$$\Phi(r,z) \geqq 0 \quad \text{for } 1 \leqq r,\quad 0 \leqq z \leqq 1. \tag{3.3}$$

On the other hand, due to the boundary condition on the initial data u_0 in (2.2), one can use the first equation in (1.1) with $\nu = 0$ to solve u:

$$u^2(t,r,z) = u_0^2(r,z)\exp\left\{4\int_0^t \partial_z\psi(s,r,z)\,\mathrm{d}s\right\} \quad \text{for } z \neq 0, 1.$$

Hence, by continuity, as long as the solution is smooth, one also has

$$u(t,r,0) = u(t,r,1) = 0. \tag{3.4}$$

Multiplying the second equation in (1.1) with $\nu = 0$ by ϕ_z and integrating over $\Omega(1,\infty)$, we have

$$-\int_0^1\int_1^\infty \left(\partial_r^2 + \frac{3}{r}\partial_r + \partial_z^2\right)\psi_t\phi_z r^3\,\mathrm{d}r\,\mathrm{d}z = \int_0^1\int_0^\infty \partial_z u^2\phi_z r^3\,\mathrm{d}r\,\mathrm{d}z. \tag{3.5}$$

On the one hand, using (3.4) and performing integration by parts, we get

$$\int_0^1\int_1^\infty \partial_z u^2\phi_z r^3\,\mathrm{d}r\,\mathrm{d}z = -\int_0^1\int_1^\infty u^2\partial_z^2\phi r^3\,\mathrm{d}r\mathrm{d}z = \pi^2\int_0^1\int_1^\infty u^2\phi r^3\,\mathrm{d}r\,\mathrm{d}z. \tag{3.6}$$

On the other hand, using the boundary condition (2.3) and performing integration by parts, we obtain by noting that $\theta_r(1) + \beta\theta(1) = 0$ that

$$\begin{aligned}
&-\int_0^1\int_1^\infty \left(\partial_r^2 + \frac{3}{r}\partial_r + \partial_z^2\right)\psi_t\phi_z r^3\,\mathrm{d}r\,\mathrm{d}z \\
&= \frac{\mathrm{d}}{\mathrm{d}t}\int_0^1 (\psi_r\phi_z - \psi\partial_{rz}^2\phi)|_{r=1}\,\mathrm{d}z - \frac{\mathrm{d}}{\mathrm{d}t}\int_0^1\int_1^\infty \psi\left(\partial_r^2 + \frac{3}{r}\partial_r\right)\phi_z r^3\,\mathrm{d}r\,\mathrm{d}z \\
&\quad + \frac{\mathrm{d}}{\mathrm{d}t}\int_0^1\int_1^\infty \psi_z\partial_z^2\phi r^3\,\mathrm{d}r\,\mathrm{d}z \qquad (3.7)\\
&= \pi\theta(1)\frac{\mathrm{d}}{\mathrm{d}t}\int_0^1 (\cos\pi z)(\psi_r + \beta\psi)|_{r=1}\,\mathrm{d}z + \frac{\mathrm{d}}{\mathrm{d}t}\int_0^1\int_1^\infty \psi_z\Phi r^3\,\mathrm{d}r\,\mathrm{d}z \\
&= \frac{\mathrm{d}}{\mathrm{d}t}\int_0^1\int_1^\infty \psi_z\Phi r^3\,\mathrm{d}r\,\mathrm{d}z. \qquad (3.8)
\end{aligned}$$

Combining (3.7) with (3.5)–(3.6) gives

$$\frac{\mathrm{d}}{\mathrm{d}t}\int_0^1\int_1^\infty \psi_z\Phi r^3\,\mathrm{d}r\mathrm{d}z = \pi^2\int_0^1\int_1^\infty u^2\phi r^3\,\mathrm{d}r\mathrm{d}z. \tag{3.9}$$

Multiplying the first equation in (1.1) with $\nu = 0$ by Φ and integrating on $\Omega(1,\infty)$ yield

$$\frac{\mathrm{d}}{\mathrm{d}t}\int_0^1\int_1^\infty (\log u^2)\Phi r^3\,\mathrm{d}r\mathrm{d}z = 4\int_0^1\int_1^\infty \psi_z\Phi r^3\,\mathrm{d}r\mathrm{d}z. \tag{3.10}$$

Since $\int_0^1 \int_1^\infty \partial_z \psi_0 \Phi r^3 \, dr dz > 0$, we conclude from (3.9) that

$$\int_0^1 \int_1^\infty \psi_z \Phi r^3 \, dr dz > 0 \quad \text{for all } t \geqq 0. \tag{3.11}$$

By using (3.2), we obtain

$$\begin{aligned}
&\int_0^1 \int_1^\infty (\log u^2) \Phi r^3 \, dr dz \leqq \int_0^1 \int_1^\infty (\log^+ u^2) \Phi r^3 \, dr dz \\
&\leqq 2 \int_0^1 \int_1^\infty |u| \Phi r^3 \, dr dz \\
&\leqq 2 \left(\int_0^1 \int_1^\infty |u|^2 \phi r^3 \, dr dz \right)^{\frac{1}{2}} \left(\int_0^1 \int_1^\infty (\Phi/\phi)^2 \phi r^3 \, dr dz \right)^{\frac{1}{2}} \\
&\leqq c_0 \left(\int_0^1 \int_1^\infty |u|^2 \phi r^3 \, dr dz \right)^{\frac{1}{2}},
\end{aligned} \tag{3.12}$$

where c_0 is defined by

$$c_0 = 2 \left\{ \int_0^1 \int_1^\infty \left(4\alpha^2 r^2 - (8\alpha + \pi^2) \right)^2 \phi r^3 \, dr dz \right\}^{\frac{1}{2}} < \infty. \tag{3.13}$$

Let

$$X(t) \equiv \int_0^1 \int_1^\infty \psi_z \Phi r^3 \, dr dz, \quad Y(t) \equiv \int_0^1 \int_1^\infty (\log u^2) \Phi r^3 \, dr dz. \tag{3.14}$$

Using (3.9) and (3.10), we get

$$\frac{d}{dt} Y(t) = 4X(t), \tag{3.15}$$

and

$$\frac{d^2}{dt^2} Y(t) = 4\pi^2 \int_0^1 \int_1^\infty u^2 \phi r^3 \, dr dz. \tag{3.16}$$

Integrating (3.16) twice in time and using (3.15), we obtain

$$Y(t) = Y(0) + 4X(0)t + 4\pi^2 \int_0^t \int_0^s \int_0^1 \int_1^\infty u^2(\tau, r, z) \phi r^3 \, dr \, dz \, d\tau \, ds. \tag{3.17}$$

By our assumption, we have $X(0) > 0$ and $Y(0)$ is finite. Define $m_0 = \max\{-Y(0), 0\}$ and $t_1 = \frac{m_0}{4X(0)} \geqq 0$. Then we get

$$Y(0) + 4X(0)t_1 \geqq -m_0 + 4X(0)t_1 = 0. \tag{3.18}$$

Thus, we obtain for $t \geqq t_1$ that

$$\begin{aligned} Y(t) &= Y(0) + 4X(0)t_1 + 4X(0)(t-t_1) \\ &\quad + 4\pi^2 \int_0^t \int_0^s \int_0^1 \int_1^\infty u^2(\tau, r, z)\phi r^3 \, \mathrm{d}r\mathrm{d}z\mathrm{d}\tau\mathrm{d}s \\ &\geqq 4X(0)(t-t_1) + 4\pi^2 \int_{t_1}^t \int_{t_1}^s \int_0^1 \int_1^\infty u^2(\tau, r, z)\phi r^3 \, \mathrm{d}r\mathrm{d}z \, \mathrm{d}\tau \, \mathrm{d}s. \end{aligned} \tag{3.19}$$

Substituting (3.12) into (3.19), we obtain the following estimate for $t \geqq t_1$:

$$\begin{aligned} \left(\int_0^1 \int_1^\infty u^2(t, r, z)\phi r^3 \, \mathrm{d}r\mathrm{d}z \right)^{1/2} &\geqq \frac{4X(0)(t-t_1)}{c_0} \\ &\quad + \frac{4\pi^2}{c_0} \int_{t_1}^t \int_{t_1}^s \int_0^1 \int_1^\infty u^2(\tau, r, z)\phi r^3 \\ &\quad \times \mathrm{d}r \, \mathrm{d}z \, \mathrm{d}\tau \, \mathrm{d}s. \end{aligned} \tag{3.20}$$

For $t \geqq t_1$, we define

$$F(t) = \frac{4X(0)(t-t_1)}{c_0} + \frac{4\pi^2}{c_0} \int_{t_1}^t \int_{t_1}^s \int_0^1 \int_1^\infty u^2(\tau, r, z)\phi r^3 \, \mathrm{d}r \, \mathrm{d}z \, \mathrm{d}\tau \, \mathrm{d}s. \tag{3.21}$$

Then we have $F(t_1) = 0$ and $F_t(t_1) = \frac{4X(0)}{c_0} > 0$. By differentiating (3.21) twice in time and substituting the resulting equation into (3.20), we obtain

$$\frac{\mathrm{d}^2 F}{\mathrm{d}t^2} = \frac{4\pi^2}{c_0} \int_0^1 \int_1^\infty u^2(t, r, z)\phi r^3 \, \mathrm{d}r\mathrm{d}z \geqq DF^2, \tag{3.22}$$

where $D = \frac{4\pi^2}{c_0}$. Clearly, we have $F_t > 0$ for $t \geqq t_1$. Multiplying F_t to (3.22) and integrating from t_1 to t, we get

$$\frac{\mathrm{d}F}{\mathrm{d}t} \geqq \sqrt{\frac{2D}{3}F^3 + C}, \tag{3.23}$$

where $C = (F_t(t_1))^2 = (\frac{4X(0)}{c_0})^2 > 0$. Let

$$I(x) = \int_0^x \frac{\mathrm{d}y}{\sqrt{y^3+1}}, \quad J = \left(\frac{3C}{2D} \right)^{1/3}.$$

Then, integrating (3.23) from t_1 to t gives

$$I\left(\frac{F(t)}{J} \right) \geqq \frac{\sqrt{C}(t-t_1)}{J}, \quad \forall t \geqq t_1. \tag{3.24}$$

Note that both I and F are strictly increasing functions, and $I(x)$ is uniformly bounded for all $x > 0$ while the right hand side increases linearly in time. It follows from (3.24) that $F(t)$ must blow up no later than

$$T^* = t_1 + \frac{J}{\sqrt{C}} I_\infty = \frac{m_0}{4X(0)} + \left(\frac{3c_0^2}{32X(0)\pi^2} \right)^{1/3} I_\infty, \tag{3.25}$$

where $I_\infty = \int_0^\infty \frac{\mathrm{d}y}{\sqrt{y^3+1}} < \infty$. This contradicts the assumption that the 3D inviscid model has a globally smooth solution. This contradiction implies that the 3D inviscid model with the initial boundary conditions considered in Theorem 2.2 must develop a finite time singularity no later than T^*. This completes the proof of Theorem 2.2. □

4. Numerical Confirmation of the Finite Time Blowup

In this section we provide numerical evidence on the finite time blowup of the 3D inviscid model (1.1) in the interior domain. Specifically, we numerically solve (1.1) on the cylinder $\Omega(0, 1)$ using the initial data:

$$u_0 = 300(1 - r^2)^{40} \sin^{20}(\pi z), \tag{4.1a}$$

$$\psi_0 = -10(1 - r^2)(1 - z)\mathrm{e}^{(1-\beta)z}, \tag{4.1b}$$

together with (i) the Dirichlet-Robin type boundary condition (2.10):

$$\psi|_{r=1} = 0, \quad \psi|_{z=1} = 0, \quad (\psi_z + \beta\psi)|_{z=0} = 0,$$

and (ii) the *energy-conserving* homogeneous boundary condition:

$$\psi|_{r=1} = 0, \quad \psi|_{z=0} = 0, \quad \psi|_{z=1} = 0. \tag{4.2}$$

For the Dirichlet-Robin boundary condition (2.10), the parameter β is taken to be $\beta = 4.87$, which roughly corresponds to the choice $\alpha = 3$ (cf. (2.9)). The purpose of our experiment is to demonstrate the finite time blowup of the 3D model (1.1) under *both* boundary conditions, and to understand the driving mechanism behind these blowups.

4.1. The Numerical Method

The Equation (1.1) is discretized on an adaptive mesh using a standard 4th-order finite difference scheme, and is integrated in time using the explicit 4th-order Runge–Kutta method. The time step is chosen dynamically so that in each step the relative change of the solution does not exceed a certain threshold, say 5 %. The adaptive mesh is constructed from a pair of analytic mesh mapping functions (one in r, one in z), whose parameters are automatically adjusted during the simulation so that roughly 50 % of the mesh points are placed in the "peak" region where the solution is most singular (see Fig. 5 for an illustration of the mesh used in z). The detailed construction and update of the adaptive mesh will be reported in a forthcoming paper, and hence will be omitted here.

4.2. Overview of the Numerical Results

All computations presented in this section are performed on a 512×512 "coarse" mesh and a $1{,}024\times1{,}024$ "fine" mesh. In each computation, the solution is advanced indefinitely in time until the time step drops below 10^{-12}. For computations using the Dirichlet-Robin boundary condition (2.10), the stop time t_e and the corresponding time steps Δt are listed in Table 1. For computations using the homogeneous boundary condition (4.2), similar results are reported in Table 2. It can be observed from these tables that: (i) for each computation, there exists a short time interval right before the stop time t_e (t_e') in which the solution increases rapidly: this can be readily inferred from the sharp decrease of the time step Δt; (ii) the rapid growth of the solution is more evident for the high resolution ($1{,}024\times1{,}024$) runs, which can be deduced from the earlier stop time t_e (t_e') in these cases. As will be made clear in what follows, these scenarios are precursors of the *finite time blowup* of the solution that is about to take place (cf. Fig. 1a, 2, 3).

Table 1. Stop time t_e and corresponding time steps Δt for computations using the Dirichlet-Robin boundary condition (2.10)

Mesh size	t_e	Δt at t_e	Δt at $t = 0.0389$
512×512	0.0389130	7.4029×10^{-13}	2.5702×10^{-7}
$1{,}024 \times 1{,}024$	0.0389084	8.8433×10^{-13}	1.5778×10^{-7}

Table 2. Stop time t_e' and corresponding time steps Δt for computations using the homogeneous boundary condition (4.2)

Mesh size	t_e'	Δt at t_e'	Δt at $t = 0.04731$
512×512	0.0473207	9.7949×10^{-13}	1.4079×10^{-7}
$1{,}024 \times 1{,}024$	0.0473186	9.0729×10^{-13}	1.7740×10^{-7}

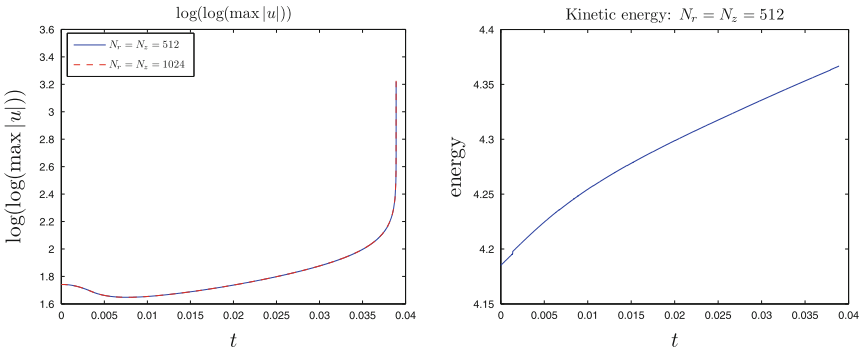

(a) $\log(\log\|u(\cdot,t)\|_\infty)$ **(b)** kinetic energy E

Fig. 1. The finite-energy, finite time blowup of the solution generated by the Dirichlet-Robin boundary condition (2.10): **a** $\log(\log\|u(\cdot,t)\|_\infty)$; **b** kinetic energy E. In **a** the results from both the 512×512 and the $1{,}024\times1{,}024$ resolutions are shown, but the *curves* overlap and are virtually indistinguishable from each other

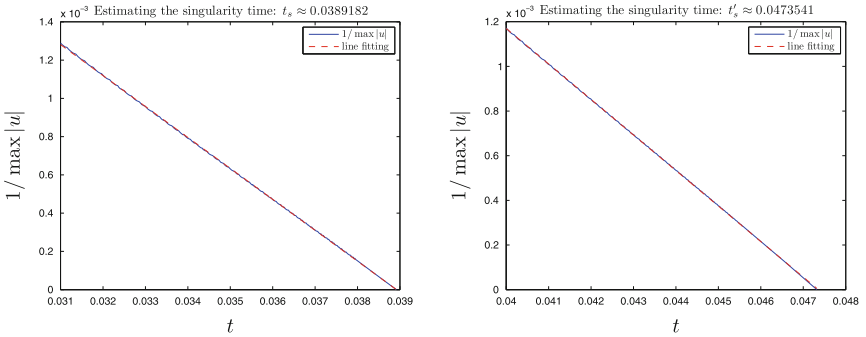

(a) Dirichlet-Robin: $N_r = N_z = 512$ **(b)** homogeneous: $N_r = N_z = 512$

Fig. 2. Estimate of singularity time based on line fitting for $1/\|u(\cdot,t)\|_\infty \approx c_0(t_s - t)$. **a** Dirichlet-Robin boundary condition (2.10): the fitting yields $t_s \approx 0.0389182$ for coarse mesh data and $t_s \approx 0.0389096$ for fine mesh data (not shown); **b** homogeneous boundary condition (4.2): the fitting yields $t'_s \approx 0.0473541$ for coarse mesh data and $t'_s \approx 0.0473521$ for fine mesh data (not shown). In both plots the data $1/\|u(\cdot,t)\|_\infty$ is overlaid with the fitted line, which are virtually indistinguishable from each other

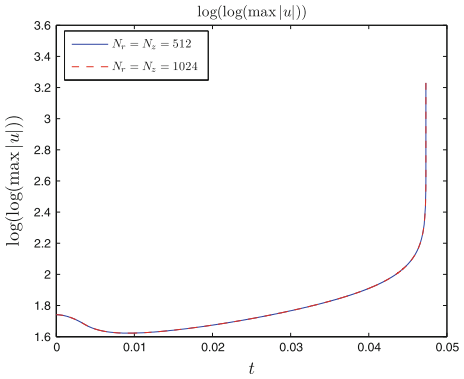

Fig. 3. The finite time blowup of the solution generated by the homogeneous boundary condition (4.2), indicated by the unbounded growth of $\log(\log\|u(\cdot,t)\|_\infty)$. The results from both the 512×512 and the $1{,}024 \times 1{,}024$ resolutions are shown, but the *curves* overlap and are virtually indistinguishable from each other

Table 3. Effective mesh resolutions N_r^{eff}, N_z^{eff} near $\|u(\cdot,t)\|_\infty$ at $t = 0.038$, for computations using the Dirichlet-Robin boundary condition (2.10) (cf. Fig. 5b)

Mesh size	N_r^{eff}	N_z^{eff}
512×512	1.8620×10^4	5.4162×10^3
$1{,}024 \times 1{,}024$	3.7163×10^4	1.0926×10^4

To see how well the solution is resolved in regions where it is most singular, we also report in Tables 3, 4 the effective mesh resolutions N_r^{eff}, N_z^{eff} used in each computation near the maximum of u, $\|u(\cdot,t)\|_\infty$, for selected time instants t close to the stop time t_e (t'_e).

Table 4. Effective mesh resolutions N_r^{eff}, N_z^{eff} near $\|u(\cdot,t)\|_\infty$ at $t = 0.046$, for computations using the homogeneous boundary condition (4.2) (cf. Fig. 5d)

Mesh size	N_r^{eff}	N_z^{eff}
512×512	1.8079×10^4	4.9889×10^3
$1{,}024 \times 1{,}024$	3.6641×10^4	1.0223×10^4

It turns out that, for both boundary conditions (2.10) and (4.2), the 512×512 coarse mesh computation and the $1{,}024 \times 1{,}024$ fine mesh computation yield very similar results. For instance, for computations using the Dirichlet-Robin boundary condition (2.10), the relative error of $\|u(\cdot,t)\|_\infty$ between the two resolutions is less than 2.82 % up to $t = 0.038$. As for computations using the homogeneous boundary condition (4.2), the relative error of $\|u(\cdot,t)\|_\infty$ between the two resolutions is less than 0.55 % up to $t = 0.046$. In view of these small differences, in the presentation below only the results on the coarse mesh will be shown, and the ones obtained on the fine mesh will be omitted, unless otherwise stated.

4.3. Evidence for Finite-Energy, Finite Time Blowup

We first demonstrate the finite-energy, finite time blowup of the solution generated by the Dirichlet-Robin boundary condition (2.10). Fig. 1a shows the double logarithm of the sup-norm of u, $\log(\log \|u(\cdot,t)\|_\infty)$, viewed as a function of time. It is clear from this figure that $\|u(\cdot,t)\|_\infty$ grows much faster than double exponential, and it blows up at some finite time $t_s < 0.04$. A closer examination of the data suggests that $\|u(\cdot,t)\|_\infty \sim O(t_s - t)^{-1}$, and a standard line fitting procedure yields $t_s \approx 0.0389182$ (Fig. 2a). Note how close t_s is to $t_e = 0.0389130$.

Fig. 1b shows the kinetic energy of the solution, defined by (cf. [22])

$$E = \left\{ \frac{1}{2} \int_0^1 \int_0^1 \left(|u|^2 + 2|\psi_r|^2 + 2|\psi_z|^2 \right) r^3 \, dr \, dz \right\}^{1/2}.$$

It is evident that the energy remains essentially bounded up to the singularity time t_s, and this confirms that the blowup of the solution is *not* a result of unboundedly increasing energy (there do exist, however, finite time blowups with infinite energies, as we have discovered in our experiments).

We next demonstrate the finite time blowup of the solution generated by the homogeneous boundary condition (4.2). Fig. 3 shows the double logarithm of the sup-norm of u, $\log(\log \|u(\cdot,t)\|_\infty)$, viewed as a function of time. It is clear that $\|u(\cdot,t)\|_\infty$ again grows unboundedly and becomes infinite at some finite time $t_s' < 0.05$. A closer examination of the data suggests that $\|u(\cdot,t)\|_\infty \sim O(t_s' - t)^{-1}$, and a standard line fitting procedure yields $t_s' \approx 0.0473541$ (Fig. 2b). Note how close t_s' is to $t_e' = 0.0473207$.

To see how well the energy is conserved when the homogeneous boundary condition (4.2) is enforced, we compute the relative change $e_E(t) := (E(t) - E(0))/E(0)$ of the energy E at the stop time t_e'. The result shows that the coarse

mesh computation has a relative energy error of $e_E(t_e') \approx 3.9680 \times 10^{-4}$, and the fine mesh computation gives $e_E(t_e') \approx 9.8990 \times 10^{-5}$.[1] This clearly shows that the energy is well conserved in both computations.

4.4. Checking the Blowup Criteria

We next check that the solution generated by the Dirichlet-Robin boundary condition (2.10) satisfies the blowup criteria imposed by Theorem 2.3. First, it is easy to see that (2.9) is satisfied with the choice of the parameters $\alpha = 3,\ \beta = 4.87$. Indeed, $\sqrt{\lambda_1}$ is the first positive zero of the Bessel function J_1, which has an approximate value of $\sqrt{\lambda_1} \approx 3.8317$, so clearly $0 < \alpha < \sqrt{\lambda_1}$. With this choice of α, we have

$$\beta = \frac{\lambda_1}{\alpha} \tanh \alpha \approx 4.8698 > \sqrt{\lambda_1} \coth \sqrt{\lambda_1} \approx 3.8353,$$

so (2.9) is satisfied.

Next, it is clear that $u_0^2 > 0$ for $0 \leqq r < 1,\ 0 < z < 1$, and the weighted integrals of $\log u_0^2$ and $\psi_{0,z}$ have the values:

$$\int_0^1 \int_0^1 (\log u_0^2) \Phi r^3 \, dr \, dz \approx -166.446, \quad \int_0^1 \int_0^1 \psi_{0,z} \Phi r^3 \, dr \, dz \approx 20.659.$$

So the conditions of Theorem 2.3 are satisfied. This implies that the solution generated by (2.10) must blow up in finite time.

It is worth pointing out that the weighted integrals of $\log u_0^2$ and $\psi_{0,z}$ both increase with time. In particular, at $t = 0.0389$, the time shortly before the singularity time t_s, they take the values:

$$\int_0^1 \int_0^1 (\log u_0^2) \Phi r^3 \, dr \, dz \approx -125.8302, \quad \int_0^1 \int_0^1 \psi_{0,z} \Phi r^3 \, dr \, dz \approx 21.0756.$$

Note that the integral of $\log u_0^2$ has remained *negative* which has ensured the slow growth of the energy E. If both integrals become positive, then the energy will necessarily grow quadratically fast, as the proof of Theorem 2.3 shows.

4.5. Understanding the Blowup

So far we have demonstrated the finite time blowup of the solutions generated by both the Dirichlet-Robin boundary condition (2.10) and the homogeneous boundary condition (4.2). To understand the driving mechanism behind these blowups, we include below in Fig. 4 a representative contour plot of u and also in Fig. 5 several cross-section plots of $u,\ \psi_z$ on the symmetry axis $r = 0$. The results from both boundary conditions are shown.

[1] The energy integral is approximated using a 2nd-order trapezoidal quadrature, hence the 2nd-order convergence in its value.

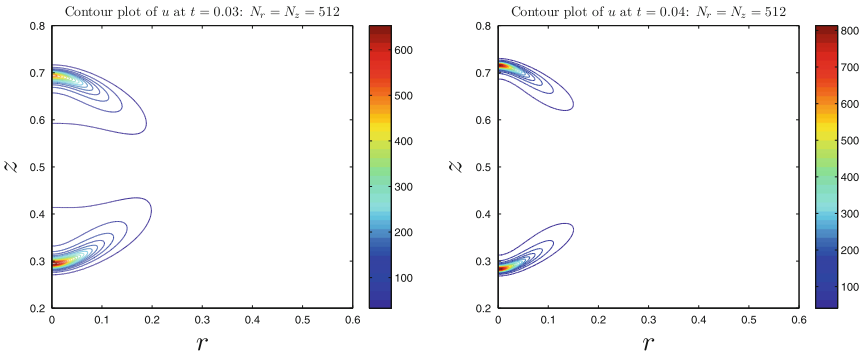

(a) Dirichlet-Robin: $t = 0.03$ **(b)** homogeneous: $t = 0.04$

Fig. 4. A representative contour plot of u. **a** Dirichlet-Robin boundary condition (2.10): $t = 0.03$; **b** homogeneous boundary condition (4.2): $t = 0.04$

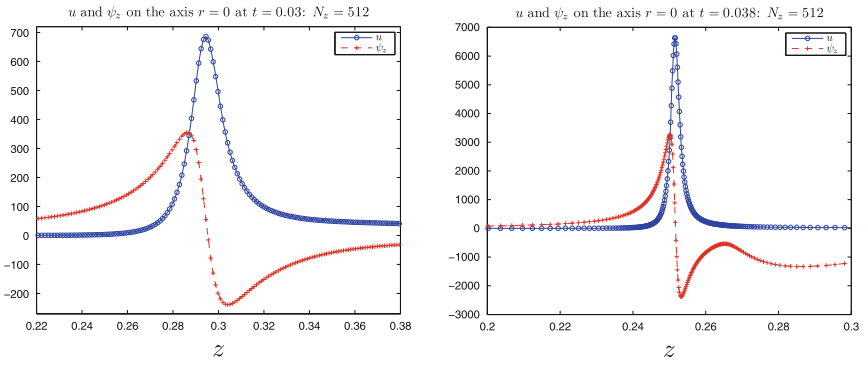

(a) Dirichlet-Robin: $t = 0.03$ **(b)** Dirichlet-Robin: $t = 0.038$

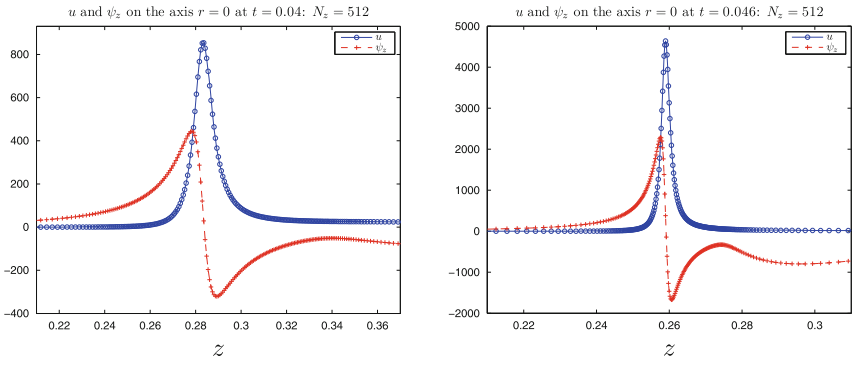

(c) homogeneous: $t = 0.04$ **(d)** homogeneous: $t = 0.046$

Fig. 5. The cross-section plots of u and ψ_z along the symmetry axis $r = 0$ near the global maximum of u. Dirichlet-Robin boundary condition (2.10): **a** $t = 0.03$; **b** $t = 0.038$; homogeneous boundary condition (4.2): **c** $t = 0.04$; **d** $t = 0.046$

To understand these figures, let's first recall that the initial data u_0 as given by (4.1a) contains a "bump" centered at the point $(r_c, z_c) = (0, 0.5)$. When the solution starts to evolve, the bump splits into two "peaks" which subsequently move away from each other (this is true regardless of the boundary condition used: see Fig. 4). Both peaks sharpen under the force of the nonlinear stretching $2u\psi_z$, and the "bottom" peak, i.e. the peak moving towards $z = 0$, grows at a faster rate and becomes singular at t_s (t_s'). The driving force behind this blowup can be readily understood from Fig. 5: near the "bottom peak" where u attains its global maximum, a good portion of the "support" of ψ_z, i.e. the region on which ψ_z is comparable to its positive maximum, overlaps the support of u, the region on which u is comparable to its positive maximum. This overlap is quite robust even when the supports of both u and ψ_z become very small (Fig. 5b, d), and it is this *nonlinear alignment* between u and ψ_z that is responsible for the formation of the finite time singularity.

Based on the above observations, it should now be clear that the finite time blowup of the solution generated by the Dirichlet-Robin boundary condition (2.10) is *not* a consequence of the boundary condition itself. Even with the homogeneous boundary condition (4.2), the solution still blows up in finite time, in much the same way as the other solution does. While the conservation of the energy enforced by (4.2) does play a role and delays the singularity time to $t_s' \approx 0.0473541$, the nonlinear alignment between u and ψ_z eventually takes over and drives the solution to infinity.

5. Global Regularity with Large Data

This section is devoted to proving Theorem 2.4.

Proof of Theorem 2.4. First of all, the local well-posedness of the initial boundary value problem can be established by using an argument similar to that of [24]. Now let us assume that (u, ψ) is a local smooth solution satisfying boundary condition (2.14) such that $u \in C([0, T); H^s(\Omega(0, 1)))$, $\psi \in C([0, T); H^{s+1}(\Omega(0, 1)))$ for some $T > 0$. We are going to show that $T = \infty$ under the assumptions of the theorem.

Denote by

$$\widetilde{v} = -\partial_z \psi, \quad \widetilde{u} = u^2.$$

It is easy to see that

$$\widetilde{v} \in C([0, T); H^s(\Omega(0, 1))), \quad \widetilde{u} \in C([0, T); H^s(\Omega(0, 1))).$$

Differentiating the second equation in (1.1) with $\nu = 0$ with respect to z, we get

$$\left(\partial_r^2 + \frac{3}{r}\partial_r + \partial_z^2\right)\partial_t \widetilde{v} = \partial_z^2 \widetilde{u}.$$

Note that $\partial_t \widetilde{v}|_{\partial\Omega(0,1)} = 0$. We define $g \equiv \Delta_5^{-1} f$ as the solution of the Laplacian equation with the homogeneous Dirichlet boundary condition:

$$\left(\sum_{i=1}^{4}\partial_{x_i}^2+\partial_z^2\right)g=f,\quad g|_{\partial\Omega(0,1)}=0,\quad \forall f\in L^2(\Omega(0,1)).$$

Then, we can reformulate the 3D inviscid model as follows:

$$\begin{cases}\widetilde{u}_t=-4\widetilde{u}\widetilde{v},\\ \widetilde{v}_t=\Delta_5^{-1}\partial_z^2\widetilde{u}.\end{cases}$$

Note that the boundary condition in (2.14) implies that

$$\widetilde{v}|_{\partial\Omega(0,1)}=M.$$

If we further denote

$$v=\widetilde{v}-M, \tag{5.1}$$

we obtain an equivalent system for $\widetilde{u}$ and v:

$$\widetilde{u}_t=-4M\widetilde{u}-4\widetilde{u}v, \tag{5.2}$$

$$v_t=\Delta_5^{-1}\partial_z^2\widetilde{u}, \tag{5.3}$$

$$v|_{\partial\Omega(0,1)}=0. \tag{5.4}$$

Recall the following well-known Sobolev inequality [14]. Let $u, v\in H^s(\Omega)$ with $s>n/2$ (n is the dimension of Ω). We have

$$\|uv\|_{H^s(\Omega)}\le C_s\|u\|_{H^s(\Omega)}\|v\|_{H^s(\Omega)}. \tag{5.5}$$

We will also use the Poincaré inequality [12]:

$$\|v\|_{H^s(\Omega)}\le C_s\|\nabla v\|_{H^{s-1}(\Omega)}, \tag{5.6}$$

if $v|_{\partial\Omega(0,1)}=0$. Here C_s is an absolute positive constant depending on s and Ω only.

Taking the H^s norm to the both sides of (5.2) and using (5.5)–(5.6), we obtain

$$\begin{aligned}\frac{\mathrm{d}}{\mathrm{d}t}\|\widetilde{u}\|_{H^s}&\leqq -4M\|\widetilde{u}\|_{H^s}+4C_s\|\widetilde{u}\|_{H^s}\|v\|_{H^s}\\ &\leqq -4M\|\widetilde{u}\|_{H^s}+4C_s^2\|\widetilde{u}\|_{H^s}\|\nabla v\|_{H^{s-1}}\\ &\leqq (-4M+4C_s^2\|\nabla v\|_{H^{s-1}})\|\widetilde{u}\|_{H^s},\end{aligned} \tag{5.7}$$

where we have used (5.6).

Next, we apply ∇ to the both sides of (5.3) and take the H^{s-1}-norm. We get

$$\begin{aligned}\frac{\mathrm{d}}{\mathrm{d}t}\|\nabla v\|_{H^{s-1}}&\leqq \|\nabla\Delta_5^{-1}\partial_z^2\widetilde{u}\|_{H^{s-1}}\\ &\leqq \|\Delta_5^{-1}\partial_z^2\widetilde{u}\|_{H^s}\\ &\leqq C_s\|\partial_z^2\widetilde{u}\|_{H^{s-2}}\leqq C_s\|\widetilde{u}\|_{H^s},\end{aligned} \tag{5.8}$$

where we have used the elliptic regularity estimate for Δ_5^{-1} in Lemma A.1.

By the local well-posedness result and the assumption on the initial condition (2.15), we know that there exists a positive $T > 0$ such that we have

$$\|\nabla v(t)\|_{H^{s-1}} \leqq \frac{M}{2C_s^2}, \quad 0 \leqq t \leqq T. \tag{5.9}$$

Let T^* be the largest time such that (5.9) holds. We will prove that $T^* = \infty$. Suppose $T^* < \infty$. Substituting (5.9) into (5.7), we obtain

$$\frac{\mathrm{d}}{\mathrm{d}t}\|\widetilde{u}\|_{H^s} \leqq -2M\|\widetilde{u}\|_{H^s}, \quad 0 \leqq t < T^*, \tag{5.10}$$

which implies

$$\|\widetilde{u}\|_{H^s} \leqq \|\widetilde{u_0}\|_{H^s}\mathrm{e}^{-2Mt}, \quad 0 \leqq t < T^*. \tag{5.11}$$

Now substituting (5.11) into (5.8) yields

$$\begin{aligned} \|\nabla v\|_{H^{s-1}} &\leqq \|\nabla v_0\|_{H^{s-1}} + C_s\|\widetilde{u_0}\|_{H^s}\int_0^t \mathrm{e}^{-2Ms}\mathrm{d}s \\ &\leqq \|\nabla v_0\|_{H^{s-1}} + \frac{C_s}{2M}\|\widetilde{u_0}\|_{H^s} \\ &\leqq \frac{M}{4C_s^2} < \frac{M}{2C_s^2}, \quad 0 \leqq t < T^*, \end{aligned} \tag{5.12}$$

where we have used the condition (2.15). Since $\|\nabla v\|_{H^{s-1}} \leqq \frac{M}{4C_s^2} < \frac{M}{2C_s^2}$ for $t < T^*$ and $\|\widetilde{u}\|_{H^s} \leqq \|\widetilde{u_0}\|_{H^s}\mathrm{e}^{-2MT^*} < \|\widetilde{u_0}\|_{H^s}$ for $t < T^*$, we can use our *a priori* estimates (5.7), (5.8) to show that (5.9) remains valid for $0 \leqq t \leqq T^* + \delta$ for some $\delta > 0$. This contradicts the assumption that T^* is the largest time such that (5.9) holds. This contradiction implies that $T^* = \infty$ and estimates (5.11), (5.12) remain valid for all times. This completes the proof of Theorem 2.4. □

Acknowledgments We would like to thank the referee for making several valuable suggestions which help improve the quality of our original manuscript. This work was supported in part by NSF by Grants DMS-0908546 and DMS-1159138. Zhen Lei would like to thank the Applied and Computational Mathematics of Caltech and Prof. Thomas Hou for hosting his visit and for their hospitality during his visit. Zhen Lei was in part supported by NSFC (grant No.11171072), the Foundation for Innovative Research Groups of NSFC (grant No.11121101), FANEDD, Innovation Program of Shanghai Municipal Education Commission (grant No.12ZZ012) and SGST 09DZ2272900. The research of Dr. S. Wang was supported by China 973 Program (Grant no. 2011CB808002), the Grants NSFC 11071009 and CIT&TCD20130312.

Appendix A. Local Well-Posedness in the Exterior Domain

The local well-posedness theory of the initial-boundary value problem of the 3D inviscid model (1.1) with (2.2), (2.3) is based on Lemma A.2. Once Lemma A.2 is proved, the local well-posedness can be established in exactly the same way as

the local well-posedness analysis presented in [24]. Let us outline the key points of proof of Theorem 2.1 as follows. Denote by $\widetilde{u} = u^2$ and let $\mathcal{K} : H^2(\Omega(1,\infty)) \to H^4(\Omega(1,\infty))$ be a linear operator defined as follows: for all $\omega \in H^2$ with $\int_0^1 \omega(r,z)\,\mathrm{d}z = 0$ for $1 \le r < \infty$ and $\partial_z\omega|_{z=0,1} = 0$, $\mathcal{K}(\omega)$ is the solution of the boundary value problem

$$\begin{cases} -\left(\partial_r^2 + \frac{3}{r}\partial_r + \partial_z^2\right)\psi = \omega, \quad 1 < r < \infty,\ 0 < z < 1, \\ (\psi_r + \beta\psi)|_{r=1} = 0, \quad \psi_z|_{z=0} = 0, \quad \psi_z|_{z=1} = 0, \end{cases}$$

where $\beta \in S_{\text{exterior}}$ is a constant. It follows from Lemma A.2 that for any $\omega \in H^2(\Omega(1,\infty))$ with $\int_0^1 \omega(r,z)\mathrm{d}z = 0$ for $1 \le r < \infty$ and $\partial_z\omega|_{z=0,1} = 0$, we have

$$\|\mathcal{K}(\omega)\|_{H^4(\Omega(1,\infty))} \le C_s\|\omega\|_{H^2(\Omega(1,\infty))}.$$

Since $u_0|_{z=0,1} = u_{0z}|_{z=0,1} = 0$, we have $\int_0^1 \partial_z\widetilde{u}\mathrm{d}z = 0$ for $1 \le r < \infty$ and $\partial_z^2\widetilde{u}|_{z=0,1} = 0$ by using the equation $\partial_t\widetilde{u} = 4\widetilde{u}\partial_z\psi$. Thus, using the definition of the operator $\mathcal{K}$, we can rewrite the 3D inviscid model (1.1) with (2.2), (2.3) in the following equivalent form:

$$\begin{aligned} \partial_t\widetilde{u} &= 4\widetilde{u}\partial_z\psi,\ (r,z) \in \Omega(1,\infty), \\ \partial_t\psi &= \mathcal{K}(\partial_z\widetilde{u}),\ (r,z) \in \Omega(1,\infty), \end{aligned}$$

with the initial condition

$$(\widetilde{u},\psi)(r,z,t=0) = (u_0^2,\psi_0)(r,z),\ (r,z) \in \Omega(1,\infty).$$

Now the local existence result in Theorem 2.1 can be obtained by following the proof of Theorem 2.1 in [24].

It remains to prove Lemma A.2. We will only present the proof of Lemma A.2 in a slightly modified domain with $1 < r < \infty$ and $0 < z < \pi$. To prove Lemma A.2, we need the following elliptic estimate which is standard for a regular domain. Even though our domain has a corner, the elliptic regularity estimate is still valid by using the compatibility conditions of ω at the corner, which can be guaranteed by the ones of the initial data at the boundary (see the assumptions on the initial data u_0 in Theorems 2.1, 2.3 and 2.4).

Consider the elliptic equation

$$-\left(\partial_r^2 + \frac{3}{r}\partial_r + \partial_z^2\right)v = f, \quad z \in [0,\pi], \tag{A.1}$$

with the boundary condition

$$v(r,0) = 0,\ v(r,\pi) = 0,\ 0 \le r \le 1, \quad v(1,z) = 0, \tag{A.2}$$

in the interior domain $\Omega = \{(r,z) \mid r \le 1,\ 0 \le z \le \pi\}$ and

$$v(r,0) = 0,\ v(r,\pi) = 0,\ 1 \le r < \infty, \quad v(1,z) = 0, \quad v(r,z) \to 0 \text{ as } r \to \infty \tag{A.3}$$

or

$$v_z(r,0)=0,\ v_z(r,\pi)=0,\ 1\le r<\infty,\quad v(1,z)=0,\quad v(r,z)\to 0 \text{ as } r\to\infty \tag{A.4}$$

in the exterior domain $\Omega=\{(r,z)\mid 1\le r<\infty,\ 0\le z\le\pi\}$.

We will focus on the exterior domain problem and use the following notations: $\|f\|_{L^2}^2=\int_0^\pi\int_1^\infty f(x,z)^2r^3\,\mathrm{d}r\mathrm{d}z$, $\|f(\cdot,z)\|_{L^2_x}^2=\int_1^\infty f(r,z)^2r^3\mathrm{d}r$. Similar notations for H^1 are also applied.

Lemma A.1. *(i) Let $f\in H^m$ with $m\geqq 0$. Further, we assume that $\partial_z^{(2k)}f|_{z=0}=0$ and $\partial_z^{(2k)}f|_{z=\pi}=0$ for all integers $k=0,\dots,[\frac{m-1}{2}]$ if $m\ge 1$. Then there exists a unique solution $v\in H^{m+2}$ to (A.1) with the boundary condition (A.2) or (A.3), satisfying*

$$\|v\|_{H^{m+2}}\le C\|f\|_{H^m} \tag{A.5}$$

for some generic constant $C>0$.

(ii) Let $f\in H^m$ with $m\geqq 0$ satisfying $\int_0^\pi f(r,z)\mathrm{d}z=0$ for $1\le r<\infty$. Furthermore, we assume that $\partial_z^{(2k+1)}f|_{z=0}=0$ and $\partial_z^{(2k+1)}f|_{z=\pi}=0$ for all integers $k=0,\dots,[\frac{m-2}{2}]$ if $m\ge 2$. Then there exists a unique solution $v\in H^{m+2}$ to (A.1) with the boundary condition (A.4) satisfying

$$\|v\|_{H^{m+2}}\le C\|f\|_{H^m} \tag{A.6}$$

for some generic constant $C>0$.

Remark A.1. Part (i) of Lemma A.1 can be proved by performing Fourier Cosine Transform in z and using a standard energy estimate. The compatibility condition on f enables us to establish the relevant Parseval equality that expresses the Sobolev norm of a function in terms of the weighted discrete sum of its Fourier Cosine Transform coefficients. Alternatively, as suggested by the referee, one can obtain these estimates by considering the Laplace equation for functions which are periodic and even in z. The boundary condition can then be imposed only on $r=1$ (on a smooth domain of the form $U=(R^4\backslash B_1)\times\{\text{circle}\}$). The estimates are consequences of the standard elliptic theory. Part (ii) of Lemma A.1 can be proved similarly by performing a Fourier Sine Transform, or by considering the Laplace equation for functions which are periodic and odd in z.

Lemma A.2. *For any given $\omega\in H^{s-2}(\Omega(1,\infty))$ with $s\geqq 4$, $\int_0^\pi\omega(r,z)\mathrm{d}z=0$ for $1\le r<\infty$, and $\partial_z^{(2k+1)}\omega|_{z=0}=\partial_z^{(2k+1)}\omega|_{z=\pi}=0$ for all integers $k=0,\dots,[\frac{s-4}{2}]$ if $s\ge 4$, there exists a unique solution $\psi\in H^s(\Omega(1,\infty))$ to the boundary value problems*

$$\begin{cases}-\big(\partial_r^2+\frac{3}{r}\partial_r+\partial_z^2\big)\psi=\omega,\quad 1<r,\ 0<z<\pi,\\ (\psi_r+\beta\psi)|_{r=1}=0,\quad \psi_z|_{z=0}=0,\quad \psi_z|_{z=\pi}=0,\end{cases} \tag{A.7}$$

where $\beta \in S_{\text{exterior}}$ is a constant. Furthermore, we have the following estimate:

$$\|\psi\|_{H^s(\Omega(1,\infty))} \leqq C\|\omega\|_{H^{s-2}(\Omega(1,\infty))}, \tag{A.8}$$

where C is an absolute positive constant.

Proof. To prove Lemma A.2, we decompose $\psi = \psi^{(1)} + \psi^{(2)}$, where $\psi^{(1)}$ is the solution of the elliptic equation with the following mixed Dirichlet–Neumann boundary condition:

$$\begin{cases} -(\partial_r^2 + \frac{3}{r}\partial_r + \partial_z^2)\psi^{(1)} = \omega, \quad \text{in } \Omega(1,\infty), \\ \psi_z^{(1)}|_{z=0} = 0, \ \psi_z^{(1)}|_{z=\pi} = 0, \ \psi^{(1)}|_{r=1} = 0, \quad \psi^{(1)} \to 0 \text{ as } r \to \infty. \end{cases} \tag{A.9}$$

Then $\psi^{(2)}$ satisfies

$$\begin{cases} -(\partial_r^2 + \frac{3}{r}\partial_r + \partial_z^2)\psi^{(2)} = 0, \quad \text{in}\Omega(1,\infty), \\ [\psi_r^{(2)} + \beta\psi^{(2)}]|_{r=1} = -\psi_r^{(1)}|_{r=1}, \\ \psi_z^{(2)}|_{z=0} = 0, \quad \psi_z^{(2)}|_{z=\pi} = 0. \end{cases} \tag{A.10}$$

The elliptic estimate (ii) with $m = s-2$ in Lemma A.1 gives $\psi^{(1)} \in H^s(\Omega(1,\infty))$ and $\|\psi^{(1)}\|_{H^s(\Omega(1,\infty))} \leqq \|\omega\|_{H^{s-2}(\Omega(1,\infty))}$. It remains to show that the Neumann-Robin problem (A.10) is well-posed.

Applying the Cosine transform to (A.10) with respect to z variable, we obtain

$$\begin{cases} -(\partial_r^2 + \frac{3}{r}\partial_r)\widehat{\psi}^{(2)} + k^2\widehat{\psi}^{(2)} = 0, \\ [\widehat{\psi}_r^{(2)} + \beta\widehat{\psi}^{(2)}]|_{r=1} = -\widehat{\psi}_r^{(1)}(1,k), \end{cases} \tag{A.11}$$

where the Cosine transform $\widehat{\cdot}$ is defined as:

$$\widehat{\psi}^{(2)}(r,k) = \sqrt{\frac{2}{\pi}} \int_0^\pi \psi^{(2)}(r,z)\cos(kz)\mathrm{d}z. \tag{A.12}$$

Let $\widehat{\psi}^{(2)}(r,k) = \frac{1}{r}h(rk,k)$. Then (A.11) can be written in terms of h as

$$k^2\frac{\mathrm{d}^2}{\mathrm{d}r^2}h(rk) + \frac{k}{r}\frac{\mathrm{d}}{\mathrm{d}r}h(rk) - \left(k^2 + \frac{1}{r^2}\right)h(rk) = 0,$$

which is equivalent to the following modified Bessel equation

$$r^2h''(r,k) + rh'(r,k) - (1+r^2)h(r,k) = 0.$$

The general solution of the modified Bessel equation with the decaying property as $r \to \infty$ is given by modified Bessel function:

$$h(r,k) = C(k)K(r),$$

where $K(r)$ is the modified Bessel function and can be represented in an integration form as follows

$$K(r) = \int_0^\infty \mathrm{e}^{-r\cosh(\theta)}\cosh(\theta)\mathrm{d}\theta, \quad K(r) \to 0 \text{ as } r \to \infty.$$

In fact, we have $0 < K(r) \leqq c_2 r^{-1/2}\mathrm{e}^{-r}$ as $r \to \infty$ for some positive constant c_2. Thus, the general solution of $\widehat{\psi}^{(2)}(k,r)$ is given by

$$\widehat{\psi}^{(2)}(r,k) = \frac{C(k)}{r} K(rk). \tag{A.13}$$

The boundary condition of $\psi^{(2)}$ in (A.11) can be used to determine $C(k)$ as follows:

$$C(k) = \frac{-\beta \widehat{\psi}^{(1)}(1,k)}{(\beta-1)K(k) + kK'(k)}. \tag{A.14}$$

Note that $C(k)$ in (A.14) is well-defined for $\beta \in S_{\text{exterior}}$. The remaining part of the proof is exactly the same as in [24]. We can show that $\psi^{(2)}$ will have the same regularity property as $\psi^{(1)}$. This proves our lemma. We will omit the details here. □

References

1. Bardos, C., Titi, E.: Euler equations for incompressible ideal fluids. *Uspekhi Mat. Nauk* **62**3(375), 5–46 (2007)
2. Beale, J.T., Kato, T., Majda, A.: Remarks on the breakdown of smooth solutions for the 3-D Euler equations. *Comm. Math. Phys.* **94**(1), 61–66 (1984)
3. Boratav, O.N., Pelz, R.B.: Direct numerical simulation of transition to turbulence from a high-symmetry initial condition. *Phys. Fluids* **6**, 2757–2784 (1994)
4. Caffarelli, L., Kohn, R., Nirenberg, L.: Partial regularity of suitable weak solutions of the Navier–Stokes equations. *Comm. Pure Appl. Math.* **35**, 771–831 (1982)
5. Caflisch, R., Siegel, M.: A semi-analytic approach to Euler singularities. *Methods Appl. Anal.* **11**, 423–430 (2004)
6. Chae, D.: On the finite-time singularities of the 3D incompressible Euler equations. *Comm. Pure Appl. Math*. **60**, 597–617 (2007)
7. Constantin, P.: Note on loss of regularity for solutions of the 3D incompressible Euler and related equations. *Commun. Math. Phys.* **104**, 311–326 (1986)
8. Constantin, P.: On the Euler equations of incompressible fluids. *Bull. Am. Math. Soc.* **44**, 603–621 (2007)
9. Constantin, P., Fefferman, C., Majda, A.: Geometric constraints on potentially singular solutions for the 3-D Euler equation. *Comm. PDEs*. **21**, 559–571 (1996)
10. Deng, J., Hou, T.Y., Yu, X.: Geometric properties and non-blowup of 3-D incompressible Euler flow. *Comm. PDEs.* **30**, 225–243 (2005)
11. Deng, J., Hou, T.Y., Yu, X.: Improved geometric conditions for non-blowup of 3D incompressible Euler equation. *Comm. PDEs.* **31**, 293–306 (2006)
12. Evans, L.C.: *Partial Differential Equations*. American Mathematical Society Publ. (1998)
13. Fefferman, C.: http://www.claymath.org/millennium/Navier-Stokesequations
14. Foland, G.B.: *Introduction to Partial Differential Equations*. Princeton University Press, Princeton (1995)
15. Grauer, R., Sideris, T.: Numerical computation of three dimensional incompressible ideal fluids with swirl. *Phys. Rev. Lett.* **67**, 3511–3514 (1991)
16. Grafke, T., Grauer, R.: Finite-time Euler singularities: a Lagrangian perspective. *Appl. Math. Lett.* **26**, 500–505 (2013)
17. Grauer, R., Marliani, C., Germaschewski, K.: Adaptive mesh refinement for singular solutions of the incompressible Euler equations. *Phys. Rev. Lett.* **80**, 4177–4180 (1998)
18. Hou, T.Y.: Blow-up or no blow-up? A unified computational and analytic approach to study 3-D incompressible Euler and Navier–Stokes equations. *Acta Numer*. **18**, 277–346 (2009)
19. Hou, T.Y., Li, R.: Dynamic depletion of vortex stretching and non-blowup of the 3-D incompressible Euler equations. *J. Nonlinear Sci.* **16**(6), 639–664 (2006)

20. HOU, T.Y., LI, R.: Blowup or no blowup? The interplay between theorey and numerics. *Physica D* **237**, 1937–1944 (2008)
21. HOU, T.Y., LI, C.M.: Dynamic stability of the 3D axi-symmetric Navier–Stokes equations with swirl. *Comm. Pure Appl. Math.* **61**(5), 661–697 (2008)
22. HOU, T.Y., LEI, Z.: On the stabilizing effect of convection in three-dimensional incompressible flows. *Comm. Pure Appl. Math.* **62**(4), 502–564 (2009)
23. HOU, T.Y., LEI, Z.: On partial regularity of a 3D model of Navier–Stokes equations. *Comm. Math. Phys.* **287**, 281–298 (2009)
24. HOU, T.Y., SHI, Z., WANG, S.: On singularity formation of a 3D model for incompressible Navier–Stokes equations. *Adv. Math.* **230**, 607–641 (2012)
25. KERR, R.M.: Evidence for a singularity of the three dimensional, incompressible Euler equations. *Phys. Fluids* **5**(7), 1725–1746 (1993)
26. LIN, F.-H.: A new proof of the Caffarelli–Kohn–Nirenberg theorem. *Comm. Pure Appl. Math.* **51**(3), 241–257 (1998)
27. LUO, G., HOU, T.Y.: Potential singular solutions of the 3D incompressible Euler equations. arXiv:1310.0497v1 [physics.flu-dyn] (2013)
28. MAJDA, A.J., BERTOZZI, A.L.: *Vorticity and Incompressible Flow*. Cambridge University Press, Cambridge (2002)
29. ORLANDI, P., CARNEVALE, G.F.: Nonlinear amplification of vorticity in inviscid interaction of orthogonal Lamb dipoles. *Phys. Fluids* **19**, 057106 (2007)
30. PRODI, G.: Un teorema di unicità per le equazioni di Navier–Stokes. *Ann. Mat. Pura Appl.* **48**, 173–182 (1959)
31. PUMIR, A., SIGGIA, E.D.: Development of singular solutions to the axisymmetric Euler equations. *Phys. Fluids A* **4**, 1472–1491 (1992)
32. SERRIN, J.: The initial value problem for the Navier–Stokes equations. In: *Nonlinear Problems*, pp. 69–98. University of Wisconsin Press, Madison (1963)

Computing and Mathematical Sciences,
California Institute of Technology,
Pasadena CA 91125
USA.
e-mail: hou@cms.caltech.edu

and

School of Mathematical Sciences,
LMNS and Shanghai Key Laboratory,
for Contemporary Applied Mathematics, Fudan University,
Shanghai 200433,
People's Republic of China

and

College of Applied Sciences,
Beijing University of Technology,
Beijing 100124
People's Republic of China

and

Department of Mechanics and Aerospace Engineering,
Peking University,
Beijing 100871
People's Republic of China

(*Received March 13, 2012 / Accepted November 21, 2013*)
Published online January 9, 2014 – © Springer-Verlag Berlin Heidelberg (*2014*)